Measuring the stability of polarization orientation in high intensity laser filaments in air

A. H. Sheinfux', E. Schleifer, J. Papeer, G. Fibich, B. Ilan, and A. Zigler

Citation: Appl. Phys. Lett. **101**, 201105 (2012); doi: 10.1063/1.4767526
View online: http://dx.doi.org/10.1063/1.4767526
View Table of Contents: http://aip.scitation.org/toc/apl/101/20
Published by the American Institute of Physics

Measuring the stability of polarization orientation in high intensity laser filaments in air

A. H. Sheinfux,[1,a)] E. Schleifer,[1] J. Papeer,[1] G. Fibich,[2] B. Ilan,[3] and A. Zigler[1]
[1]*Racah Institute of Physics, Hebrew University, Jerusalem, Israel*
[2]*Department of Applied Mathematics, Tel Aviv University, Tel Aviv 69978, Israel*
[3]*School of Natural Sciences, University of California, Merced, California 95343, USA*

(Received 30 May 2012; accepted 31 October 2012; published online 13 November 2012)

We suggest a method for measuring the polarization orientation of high-intensity beams, by analyzing the damage structures on metal targets, created by laser-plasma-metal interaction. We apply our method on laser filaments and demonstrate stability and instability of the polarization orientation dynamics. Our experimental results show that the polarization orientation of linearly polarized input beams during filamentation is stable, whereas that of elliptically polarized input beams is not. The results are supported by an analytical model. © *2012 American Institute of Physics*. [http://dx.doi.org/10.1063/1.4767526]

Laser filamentation in air is a well-known phenomenon that has been extensively researched over the last decade,[1] with various applications proposed such as light detection and ranging (LIDAR),[2] pulse shortening,[2] and weather control.[3] The main effects governing filamentation are Kerr self-focusing, diffraction and plasma defocusing. While the behavior of the electric-field amplitude along the filament is relatively well understood, the polarization of the electric field along the filament is not entirely resolved. The dynamics of the electric-field polarization was discussed from a theoretical point of view by Fibich[4] and more recently by Kolesik.[5] In addition, birefringent effects in laser filaments have been previously demonstrated.[6,7] However, so far no experimental investigation of the polarization orientation along the filament has been conducted. A direct measurement inside the filament is complicated due to the high intensities (above $10^{13}\,\mathrm{W\,cm^{-2}}$) in the filament core that damage the optical devices used for the measurements.

In this letter we demonstrate a method to measure and investigate the dynamics of polarization orientation during the collapse of laser beam into a filament in air. The polarization orientation of high intensity beams is derived by examining the polarization dependent features of the damage marks created by the beam on a metal target. We expect improved understanding of the polarization dynamics will result in improved control over the filament's collapse process and thus also improved control of laser intensity and plasma density of a filament. In our approach, the damage structures created on the target placed at various distances along the propagating laser beam path serve as polarization orientation indicators. The phenomenon we use in particular is the well-known formation of femtosecond laser induced periodic surface structures (FLIPSS).[8,9] Since FLIPSS are formed near the ablation threshold of the metal, there is a significant difference in the ablation speed for slightly different intensities.[9] Therefore, the areas of higher intensity in the interference pattern are ablated at a higher rate than the lower intensity regions of the interference pattern; hence, the grating-like FLIPSS is formed. The orientation of the FLIPSS created by elliptical polarizations, except for the near-circular case, is determined by the orientation of the major axis of the polarization ellipse.

The laser in our experiment is an amplified Ti:Sa laser. 20 mJ, 100 fs pulses were passed through a $f = 4\,\mathrm{m}$ lens to create filaments at either a single shot or a 10 Hz repetition rate. The lens was used to reduce the distance of filamentation onset and to stabilize the filament. As described in earlier work,[10] tilting the lens by 20° from the beam propagation direction means two subsequent shots were hitting the same point with a $\pm 40\,\mu\mathrm{m}$ error. A $^{\lambda}/_{4}$ waveplate was used to define the initial polarization of the laser beam.

A flat stainless-steel target was positioned normal to the beam propagation, as shown in Fig. 1(a), and for each input polarization we took a set of measurements at several locations along the filament propagation direction. At each location the target was subjected to 100 shots. Figs. 1(b) and 1(c) show typical periodic structures created by this process. The characteristic grating period for FLIPSS in our measurement is ~650 nm. The metal targets were analyzed using a scanning electron microscope (SEM).

We note that while measuring polarization through FLIPSS extends the measurability to much higher intensities than other direct methodologies there is still a maximum measurable intensity. At intensities above $\sim 10^{13}\,\mathrm{W\,cm^{-2}}$ characteristic to the laser intensities in the core of the filament, the material's surface is damaged so that FLIPSS are no longer recognizable and this methodology is no longer applicable. In the context of our measurements, the only pictures where the *entire* surface is covered with FLIPSS are the images that were taken *before* the onset of filamentation, and the last images in each set that were taken *after* the filament has propagated about ~1 m and was attenuated to the point that its peak intensity was below this threshold. In other pictures, the area etched by the filament core was damaged and unrecognizable, and in those cases we took our measurements from the envelope of the filament, up to 1 mm from the center. We assert these measurements are illustrative of the polarization inside the filament mainly because in the last two measurements of each set (where the entire

a)Author to whom correspondence should be addressed. Electronic mail: co2@gmx.com.

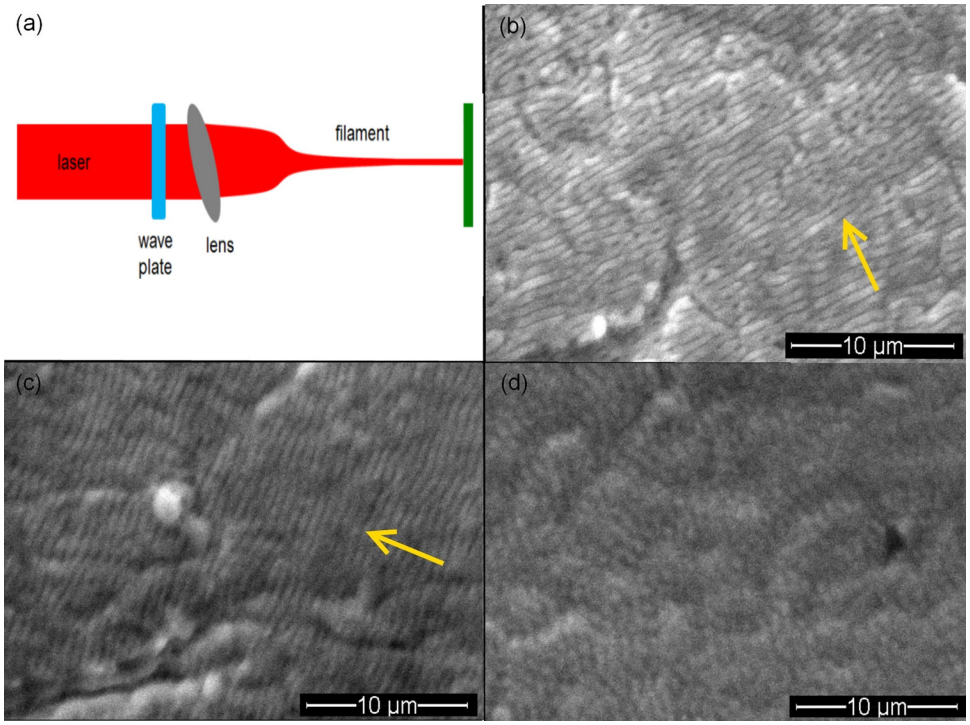

FIG. 1. System schematics. (b)–(d) Typical pictures for close- to-linear 1:4 polarization (b), elliptical 1:2 polarization (c), and close-to-circular 1:1.2 polarization (d). Yellow arrow shows the FLIPSS direction.

surface of the filament damage mark is covered in FLIPSS) we found there is no measurable difference in the FLIPSS directionality between the area enveloping the filament and the filament's center.

Fig. 2 shows the polarization orientation evolution along the filament. For a close-to-linearly-polarized input pulse ($\varphi = 32^\circ$), the polarization orientation along the filament is fairly stable. In contrast, for elliptically polarized input pulses, the polarization orientation rotates along the filament. The rotation was higher for pulses whose initial polarization state was closer to circular. The largest rotation (60°) was obtained for close-to-circular initial polarization.

Our experimental findings were supported by a theoretical model developed by us. In this model, dependency of the dynamics of the polarization orientation on initial polarization state was analyzed with the following theoretical model of two coupled weakly saturable $(2+1)$-dimensional nonlinear Schrödinger (NLS) equations:[11]

$$i\frac{\partial A_+}{\partial z} + \frac{\partial^2 A_+}{\partial x^2} + \frac{\partial^2 A_+}{\partial y^2} + \frac{2(|A_+|^2 + 2|A_-|^2)A_+}{3[1+\varepsilon(|A_+|^2 + |A_-|^2)]} = 0, \quad (1a)$$

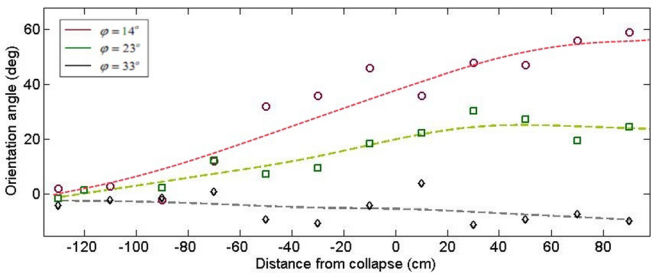

FIG. 2. Angle of FLIPSS grating vs. propagation distance. The red circles, green squares, and black rhombuses plots represent filaments created from the initial polarization of $\varphi = 14^\circ$, $\varphi = 23^\circ$, and $\varphi = 32^\circ$, respectively. The definition of φ is given in Eq. (2) so that $\varphi = 0^\circ$ and $\varphi = 45^\circ$ correspond to right-circular and linear polarizations, respectively. The dashed lines are spline interpolations.

$$i\frac{\partial A_-}{\partial z} + \frac{\partial^2 A_-}{\partial x^2} + \frac{\partial^2 A_-}{\partial y^2} + \frac{2(|A_-|^2 + 2|A_+|^2)A_+}{3[1+\varepsilon(|A_+|^2 + |A_-|^2)]} = 0, \quad (1b)$$

where $A_\pm = (A_x \pm iA_y)/\sqrt{2}$ are the pulse amplitude envelopes of the right and left circular polarization components of the electric field (accordingly), z is propagation distance, and ε is the small normalized saturation parameter. The equations were made unitless by the substitution of $x \mapsto \sqrt{\frac{n_0}{2k^2}}x$ and $z \mapsto \frac{n_0}{k}z$, where $k = \frac{2\pi}{\lambda}$ (λ is the laser wavelength) and n_0 is the air refractive index, into the wave equations. In our simulations we use $\varepsilon = 0.00025$, and an elliptically polarized input filament with a Gaussian profile

$$\begin{bmatrix} A_+(z=0,r) \\ A_-(z=0,r) \end{bmatrix} = 3.3\ e^{-r^2} \begin{bmatrix} \cos(\varphi) \\ \sin(\varphi) \end{bmatrix} \quad (2)$$

has great simplification of the overall dynamics. It captures the essential elements of the coupling between the electric field components, the Kerr nonlinearity, diffraction, and the defocusing by the plasma (which is modeled by the nonlinear saturation).

Due to the isotropy of system (1) and the radial symmetry of the input filament (2), the filament remains radially symmetric during propagation. For elliptically polarized filaments the orientation of the ellipse rotates during propagation. The angle of the semi-major axis of this ellipse with respect to the x-axis can be recovered using the Stokes' parameters as

$$\theta(z) = -\frac{1}{2}\tan^{-1}\frac{U}{Q}, \quad U = -2\mathrm{Im}\left[\int A_+^* A_- r dr\right], \quad Q = 2\mathrm{Re}\left[\int A_+^* A_- r dr\right]. \quad (3)$$

In the case of a pure linear polarization state $\varphi = 45^\circ$, the beam remains linearly polarized, and therefore the "ellipse" does not rotate. In the case of a pure circular

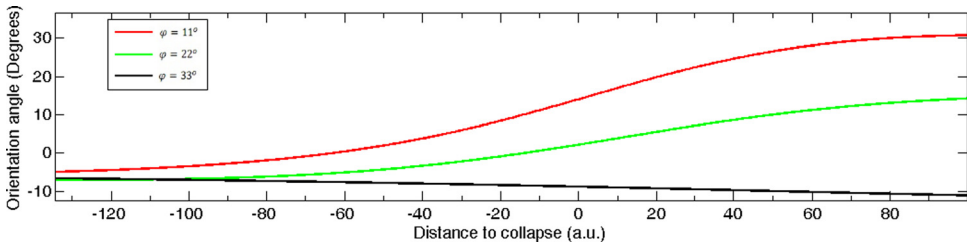

FIG. 3. Theoretical model predictions of the ellipse rotation angle [Eq. (3)] vs. normalized propagation distance, with respect to the onset of collapse, for three input polarization angles [see legend and Eq. (2)].

polarization state $\varphi = 0$, the beam remains circularly polarized. Since the major and minor axes are equal, a small departure from circular polarization will lead to fast rotations. Therefore, one can expect that the ellipse rotation velocity will increase as the polarization state changes from linear to circular. To see that, Fig. 3 shows the ellipse rotation angle vs. propagation distance predicted by the model for three different input polarizations: weak ellipticity $(\varphi = 33^\circ)$, strong ellipticity $(\varphi = 22^\circ)$, and close-to-circular $(\varphi = 11^\circ)$. One can see that

1. The more the input filament is elliptically polarized, the faster the polarization orientation rotates during propagation.
2. The polarization orientation rotates faster during the self-focusing process of the filament.

Both properties are seen to be in agreement with the experimental measurements in Fig. 2. We emphasize that Figure 3 is the result of qualitative model not a quantitative one and should be treated as such. For this reason the units in the x-axis of Fig. 3 are arbitrary.

In conclusion, we demonstrated the dynamics of polarization orientation during the collapse of a laser beam into a filament in air using FLIPSS formation. Using FLIPSS as polarization orientation diagnostics, we measured the polarization orientation at high laser beam intensities and were able to observe the evolution of the polarization orientation along the filament. For initially linearly polarized light, no significant change in the polarization orientation was observed. For initially elliptically polarized light, the polarization shifts considerably during the laser's collapse to the filament. Our model predicts the qualitative trend of the polarization orientation in the experiment.

This work was partially supported by a grant from the Israeli Science Foundation.

[1]A. Couairon and A. Mysyrowicz, Phys. Rep. **441**, 47–189 (2007).
[2]C. P. Hauri, W. Kornelis, F. W. Helbing, A. Heinrich, A. Couairon, A. Mysyrowicz, J. Biegert, and U. Keller, Appl. Phys. B **79**, 673–677 (2004).
[3]N. Khan, N. Mariun, I. Aris, and J. Yeak, New J. Phys. **4**, 61 (2002).
[4]G. Fibich and B. Ilan, Phys. Rev. E **67**, 036622 (2003).
[5]M. Kolesik, J. Moloney, and E. Wright, Phys. Rev. E **64**, 046607 (2001).
[6]C. Marceau, S. Ramakrishna, S. Génier, T.-J. Wang, Y. Chen, F. Théberge, M. Châteauneuf, J. Dubois, T. Seideman, and S. L. Chin, Opt. Commun. **283**, 2732–2736 (2010).
[7]P. Béjot, Y. Petit, L. Bonacina, J. Kasparian, M. Moret, and J. Wolf, Opt. Express **16**, 7564–7570 (2008).
[8]Y. Vorobyev, V. S. Makin, and C. Guo, J. Appl. Phys. **101**, 034903 (2007).
[9]S. Sakabe, M. Hashida, S. Tokita, S. Namba, and K. Okamuro, Phys. Rev. B **79**, 033409 (2009).
[10]G. Fibich, S. Eisenmann, B. Ilan, and A. Zigler, Opt. Lett. **29**, 1772–1774 (2004).
[11]G. P. Agrawal, *Nonlinear Fiber Optics*, 4th ed. (Academic, 2007).